Engineering Structures 32 (2010) 3516–3527

Contents lists available at ScienceDirect

Engineering Structures

journal homepage: www.elsevier.com/locate/engstruct

# Interaction of combined loads on the lateral stability of thin-walled composite beams

Sebastián P. Machado *

*Grupo Análisis de Sistemas Mecánicos, Facultad Regional Bahía Blanca, Universidad Tecnológica Nacional, 11de abril 461, B8000LMI Bahía Blanca, Argentina*
*CONICET, Argentina*

ARTICLE INFO

*Article history:*
Received 15 September 2009
Received in revised form
19 July 2010
Accepted 20 July 2010
Available online 21 August 2010

*Keywords:*
Buckling
Prebuckling deformation
Postbuckling
Thin-walled beams
Shear flexibility
Composite material

ABSTRACT

Based on a seven-degree-of-freedom shear deformable beam model, analytical solutions are derived for the lateral stability analysis of cross-ply laminated thin-walled beams subjected to combined axial and bending loads. The model includes shear deformability in a full form, i.e. shear flexibility due to both bending and nonuniform warping is considered. The theory is formulated in the context of large displacements and rotations, considering moderate bending rotations and large twist. Composite is assumed to be made of symmetric balanced laminates and especially orthotropic laminates. The closed-form analytic expressions obtained in this paper are valid for simply supported bisymmetric beams. These fundamental solutions explicitly identify the influence of geometric nonlinear effects due to the prebuckling deformation. The numerical results are compared with the bifurcation loads of the postbuckling response. In addition, the effects of the variation of load height parameter and fiber angle orientation are investigated.



## 1. Introduction

Thin-walled beam structures are major components in many engineering applications. They can be found in the design of the aircraft wing, helicopter blade, axles of vehicles and so on. Besides, composite beam members are widely used in aerospace, automobile and civil architecture industries. Among the various advantages offered by composites, it is important to mention their high strength to weight ratio, their preferred fatigue characteristics and the relatively simple techniques that are required for their production and shaping. The new generation of these constructions should be designed to work in a safe way and to experience higher performance than the conventional systems. For example, composite laminates can often sustain large elongations up to the first occurrence of localized damage; in most of the cases the failure of thin-walled composite shapes is due to elastic buckling and the load carrying capacity is directly related to the critical buckling load. Accordingly, many research activities have been conducted to the development of theoretical and computational methods for the analysis of the aforementioned structural members.

Thin-walled beams may fail in a flexural or/and torsional buckling mode: the beam suddenly deflects laterally or twists out of the plane of loading. The buckling of the beam structures is caused by the coupling among bending, twisting and stretching deformations of the beam member. Therefore, a nonlinear formulation is sometimes required for the accurate behavior prediction of such structures. The limitation of a linear buckling analysis is the omission of the prebuckling deformation. The assumption that the lateral buckling of beams is independent of the prebuckling deformations is not valid when the ratios of out-of-plane flexural and torsional stiffness to in-plane flexural stiffness are not small [1]. This effect is a relevant phenomenon in the analysis of lateral buckling which involves mechanical complications, since structures may experience large or moderately large deflections and rotations before buckling occurs.

In the classical analysis of lateral buckling of thin-walled beams, analytical solutions for critical loads were evaluated for metallic [2–4,1,5] and composite materials (for example: [6,7]). On the other hand, a few closed-form solutions have been obtained for critical loads considering the prebuckling deflections of the beam. Vacharajittiphan et al. [8] and Pi and Trahair [9] obtained an analytical solution to compute the critical loads of a simply supported doubly symmetric I-beam subjected to uniform bending. Mohri et al. [10] presented a closed-form solution to determine the critical load of a simply supported monosymmetric I-beam section under distributed load. Most of the closed-form solutions apply to slender beam where the shear deformation effects have not influence on the buckling behavior. However, the elastic couplings in an orthotropic laminate emerge from the material level that exhibits couplings between normal stress

* Tel.: +54 0291 4555220; fax: +54 0291 4555311.
*E-mail address:* smachado@frbb.utn.edu.ar.

0141-0296/$ – see front matter © 2010 Elsevier Ltd. All rights reserved.
doi:10.1016/j.engstruct.2010.07.020

and shear strain and between shear stress and normal strain. Shear deformation effect plays an important role in the behavior of the linear [6,11] and the nonlinear [12,13] stability of thin-walled composite beams. Machado and Cortínez [11,14] developed analytical expressions for the lateral buckling of composite and steel beams, which simultaneously incorporate several essential effects including higher-order bending–torsional coupling, shear deformation and warping stiffness.

To the best of the author's knowledge, there is no publication available that consider the effects of shear and prebuckling deformation on the stability response analysis of the thin-walled composite beams under combined axial and bending loads. This problem is addressed in this paper. Besides, analytical solutions are derived for the lateral stability analysis of cross-ply laminated thin-walled beams, which is an extension of others previously presented by Machado and Cortínez [11]. A compact closed-form solution was recently obtained by Mohri et al. [15]. The analytical expression includes first-order bending distribution, load height level, prebuckling deflection effects and the presence of axial loads. However, it is valid for simply supported beam–column non-shear deformable steel elements. The present model considers a geometrically nonlinear formulation to study the buckling and postbuckling behavior of thin-walled composite beams. As a distinctive feature, the present beam model incorporates, in a full form, the effects of shear flexibility (bending and warping shear). Besides, the model is presented for symmetric balanced laminates and especially orthotropic laminates. In order to perform the nonlinear analysis the Ritz variational method is used for reducing the governing equation in terms of generalized coordinates to analyze the behavior of simply supported beams under different load conditions. The buckling loads are determined from the singularity condition of the tangential stiffness matrix determinant of the structure. An incremental-iterative method based on the Newton–Raphson method combined with constant arc length is employed for the solution of nonlinear equilibrium equation. Numerical examples are presented to demonstrate the prebuckling effects and the efficiency of the proposed technique to investigate the lateral stability of thin-walled composite beams subjected to combined loads. The influences of the variation of load height parameter and fiber angle orientation are investigated. Finally, the results from the present analysis are compared with previously available results for various loading conditions.

## 2. Kinematics

A straight thin-walled composite beam with an arbitrary cross-section is considered (Fig. 1). The points of the structural member are referred to a Cartesian coordinate system $(x, \bar{y}, \bar{z})$, where the $x$-axis is parallel to the longitudinal axis of the beam while $\bar{y}$ and $\bar{z}$ are the principal axes of the cross-section. The axes $y$ and $z$ are parallel to the principal ones but having their origin at the shear center (SC), defined according to Vlasov's theory of isotropic beams. Midway through the thickness of each cross-sectional element is the middle surface. A plane perpendicular to the $x$-axis intersects the middle surface at a curve called the contour. The coordinates corresponding to points lying on the middle line are denoted as $Y$ and $Z$ (or $\bar{Y}$ and $\bar{Z}$). A contour $(n, s, x)$ coordinate system is defined with $s$ following the contour, and $n$ perpendicular to $s$. This coordinate is introduced on the middle contour of the cross-section system.

$$\bar{y}(s,n) = \bar{Y}(s) - n\frac{dZ}{ds}, \qquad \bar{z}(s,n) = \bar{Z}(s) + n\frac{dY}{ds}, \tag{1}$$

$$y(s,n) = Y(s) - n\frac{dZ}{ds}, \qquad z(s,n) = Z(s) + n\frac{dY}{ds}. \tag{2}$$

On the other hand, $y_0$ and $z_0$ are the centroidal coordinates measured with respect to the shear center.

$$\bar{y}(s,n) = y(s,n) - y_0, \qquad \bar{z}(s,n) = z(s,n) - z_0. \tag{3}$$

The present structural model is based on the following assumptions:

(1) The cross-section contour is rigid in its own plane.
(2) The warping distribution is assumed to be given by the Saint–Venant function for isotropic beams.
(3) Flexural rotations (about the $\bar{y}$ and $\bar{z}$ axes) are assumed to be moderate, while the twist $\phi$ of the cross-section can be arbitrarily large.
(4) Shell force and moment resultant corresponding to the circumferential stress $\sigma_{ss}$ and the force resultant corresponding to the shear strain in the $n$–$s$ plane ($\gamma_{ns}$) are neglected.
(5) The radius of curvature at any point of the shell is neglected.
(6) Twisting linear curvature of the shell is expressed according to the classical plate theory.
(7) The laminate stacking sequence is assumed to be symmetric and balanced, or especially orthotropic [16].

### 2.1. Development of the displacement field

According to the hypotheses of the present structural model, the displacement field proposed in Eq. (4) is based on the principle of semitangential rotation to avoid the difficulty due to the non-commutative nature of rotations [12]. In this displacement field, the torsional twist terms $\phi$ are expressed as trigonometric functions according to hypotheses (3). The displacement field is represented by means of seven degrees of freedom corresponding to three displacements ($u$, $v$ and $w$), three measures of the rotations ($\phi$, $\theta_y$ and $\theta_z$) about the shear center axis, $\bar{y}$ and $\bar{z}$ axes, respectively, and a warping variable ($\theta$) of the cross-section. The displacement field is expressed in the following form:

$$\begin{aligned} u_x &= u_o - \bar{y}\left(\theta_z\cos\phi + \theta_y\sin\phi\right) - \bar{z}\left(\theta_y\cos\phi - \theta_z\sin\phi\right) \\ &\quad + \omega\left[\theta - \frac{1}{2}\left(\theta_y'\theta_z - \theta_y\theta_z'\right)\right] + \left(\theta_z z_0 - \theta_y y_0\right)\sin\phi, \\ u_y &= v - z\sin\phi - y\left(1-\cos\phi\right) - \frac{1}{2}\left(\theta_z^2\bar{y} + \theta_z\theta_y\bar{z}\right), \\ u_z &= w + y\sin\phi - z\left(1-\cos\phi\right) - \frac{1}{2}\left(\theta_y^2\bar{z} + \theta_z\theta_y\bar{y}\right), \end{aligned} \tag{4}$$

where the prime indicates differentiation with respect to $x$. The warping function $\omega$ of the thin-walled cross-section is defined in [12]. The displacement field expression is a generalization of others previously proposed in the literature as is explained by the author in [12,14].

The components of Green's strain tensor which incorporates the large displacement are obtained as explained in [12].

## 3. Variational formulation

Taking into account the adopted assumptions, the principle of virtual work for a composite shell may be expressed in the form:

$$\begin{aligned} &\iint \left(N_{xx}\delta\varepsilon_{xx}^{(0)} + M_{xx}\delta\kappa_{xx}^{(1)} + N_{xs}\delta\gamma_{xs}^{(0)} + M_{xs}\delta\kappa_{xs}^{(1)} \right. \\ &\left. + N_{xn}\delta\gamma_{xn}^{(0)}\right)\mathrm{d}s\mathrm{d}x - \iint \left(\bar{q}_x\delta\bar{u}_x + \bar{q}_y\delta\bar{u}_y + \bar{q}_z\delta\bar{u}_z\right)\mathrm{d}s\mathrm{d}x \\ &- \iint \left(\bar{p}_x\delta u_x + \bar{p}_y\delta u_y + \bar{p}_z\delta u_z\right)|_{x=0}\mathrm{d}s\mathrm{d}n \\ &- \iint \left(\bar{p}_x\delta u_x + \bar{p}_y\delta u_y + \bar{p}_z\delta u_z\right)|_{x=L}\mathrm{d}s\mathrm{d}n \\ &- \iiint \left(\bar{f}_x\delta u_x + \bar{f}_y\delta u_y + \bar{f}_z\delta u_z\right)\mathrm{d}s\mathrm{d}n\mathrm{d}x = 0, \end{aligned} \tag{5}$$

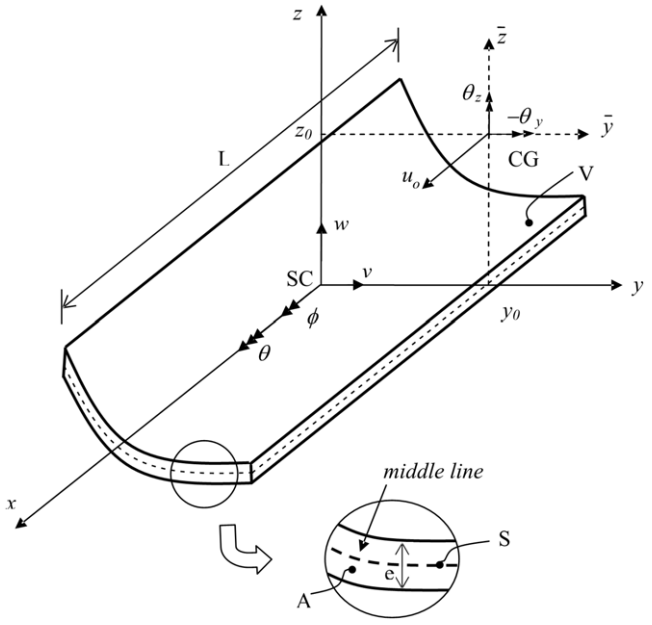


**Fig. 1.** General thin-walled section beam and notation for displacement measures.

where $N_{xx}$, $N_{xs}$, $M_{xx}$, $M_{xs}$ and $N_{xn}$ are the shell stress resultants [12]. The beam is subjected to wall surface tractions $\bar{q}_x$, $\bar{q}_y$ and $\bar{q}_z$ specified per unit area of the undeformed middle surface and acting along the $x$, $y$ and $z$ directions, respectively. Similarly, $\bar{p}_x$, $\bar{p}_y$ and $\bar{p}_z$ are the end tractions per unit area of the undeformed cross-section specified at $x = 0$ and $x = L$, where $L$ is the undeformed length of the beam. Besides $\bar{f}_x$, $\bar{f}_y$ and $\bar{f}_z$ are the body forces per unit volume. Finally, denoting $\bar{u}_x$, $\bar{u}_y$ and $\bar{u}_z$ as displacements at the middle line.

## 4. Constitutive equations

The constitutive equations of symmetrically balanced laminates may be expressed in terms of shell stress resultants in the following form [16]:

$$\begin{Bmatrix} N_{xx} \\ N_{xs} \\ N_{xn} \\ M_{xx} \\ M_{xs} \end{Bmatrix} = \begin{bmatrix} \bar{A}_{11} & 0 & 0 & 0 & 0 \\ 0 & \bar{A}_{66} & 0 & 0 & 0 \\ 0 & 0 & \bar{A}_{55}^{(H)} & 0 & 0 \\ 0 & 0 & 0 & \bar{D}_{11} & 0 \\ 0 & 0 & 0 & 0 & \bar{D}_{66} \end{bmatrix} \begin{Bmatrix} \varepsilon_{xx}^{(0)} \\ \gamma_{xs}^{(0)} \\ \gamma_{xn}^{(0)} \\ \kappa_{xx}^{(1)} \\ \kappa_{xs}^{(1)} \end{Bmatrix}, \tag{6}$$

with

$$\begin{aligned} \bar{A}_{11} &= A_{11} - \frac{A_{12}^2}{A_{22}}, \qquad \bar{A}_{66} = A_{66} - \frac{A_{26}^2}{A_{22}}, \\ \bar{A}_{55}^{(H)} &= A_{55}^{(H)} - \frac{\left(A_{45}^{(H)}\right)^2}{A_{44}^{(H)}}, \\ \bar{D}_{11} &= D_{11} - \frac{D_{12}^2}{D_{22}}, \qquad \bar{D}_{66} = D_{66} - \frac{D_{26}^2}{D_{22}}, \end{aligned} \tag{7}$$

where $A_{ij}$, $D_{ij}$ and $A_{ij}^{(H)}$ are plate stiffness coefficients defined according to the lamination theory presented by Barbero [16]. The coefficient $\bar{D}_{16}$ has been neglected because of its low value for the considered laminate stacking sequence [17].

## 5. Principle of virtual work for thin-walled beams

Substituting the deformation expressions and the constitutive equations into Eq. (5) and then integrating with respect to $s$, one obtains the one-dimensional expression for the virtual work equation given by:

$$L_K + L_P = 0, \tag{8}$$

where $L_k$ and $L_p$ represent the virtual work contributions due to the internal and external forces, respectively.

The $L_k$ and $L_p$ expressions are the same as those presented by the authors in [12]; in the same way the 1-D beam forces, in terms of the shell forces, have been defined in [12].

In the present study, the lateral buckling of beams subjected to combined axial and bending loads is considered. The applied loads are then reduced to a longitudinal force $\bar{N}$, lateral concentrated end moments $\bar{M}_y$ and uniformly distributed load $q_z$. Thus, the external work $L_p$ is defined by the following relationship:

$$L_P = \int_0^L (-q_z \delta w + \delta\phi\phi e_z q_z)\, \mathrm{d}x + \left| -\bar{N}\delta u_0 + \delta\theta_y \bar{M}_y \right|_{x=0}^{x=L}, \tag{9}$$

where

$$q_z = \int \bar{q}_z \mathrm{d}s + \iint \bar{f}_z \mathrm{d}s\mathrm{d}n, \tag{10}$$

$$\bar{M}_y = \iint \bar{p}_x \bar{z} \mathrm{d}s\mathrm{d}n, \tag{11}$$

$$\bar{N} = \iint \bar{p}_x \mathrm{d}s\mathrm{d}n, \tag{12}$$

and $e_z$ denotes the eccentricity in the $z$-direction of the applied loads from the shear center. The latter will be called the load height parameter onwards.

## 6. The discrete equilibrium problem

In order to perform the nonlinear analysis, the Ritz variational method is used to reduce the governing equation in terms of generalized coordinates. From the reduced system, first the buckling loads are determined from the singularity condition of the tangential stiffness matrix determinant of the structure. Then, an incremental-iterative method based on the Newton–Raphson method combined with constant arc length is employed for the solution of nonlinear equilibrium equation. The equations of motion are discretized to analyze the behavior of simply supported beams under different load conditions.

In this case the displacement modes are approximated by means of the following functions, which are compatible with the boundary conditions of the beam:

$$\begin{aligned} u &= U_0 \frac{x}{L}, \\ v &= v_0 \sin\left(\frac{\pi}{L}x\right), \qquad \theta_z = \theta_{z_0} \cos\left(\frac{\pi}{L}x\right), \\ w &= w_0 \sin\left(\frac{\pi}{L}x\right), \qquad \theta_y = \theta_{y_0} \cos\left(\frac{\pi}{L}x\right), \\ \phi &= \phi_0 \sin\left(\frac{\pi}{L}x\right), \qquad \theta = \theta_0 \cos\left(\frac{\pi}{L}x\right), \end{aligned} \tag{13}$$

where $U_0$, $v_0$, $w_0$, $\theta_{z0}$, $\theta_{y0}$, $\phi_0$ and $\theta_0$ are the associated displacement amplitudes.

## 7. Analytical solutions for the combined buckling

In this section, as a special case, the analytical solutions are derived for the lateral buckling of bisymmetric cross-section under combined axial and lateral loads. When the beam is loaded in its plane of symmetry it initially deflects. However, at a certain level of the applied load, the beam may buckle laterally. This phenomenon

is called lateral buckling, and the load value at which buckling occurs is the critical load. The methodology used to obtain the buckling load considering the prebuckling deformation is similar to the one developed by Machado and Cortínez in [11]. In this case, the initial displacement, corresponding to the fundamental state, is due to the state of combined load. Therefore, the prebuckling displacement components are in the form $\{u_0, v, \theta_z, w, \theta_y, \phi, \theta\}^t = \{u_0, 0, 0, w, \theta_y, 0, 0\}^t$. It is reasonable to assume that the fundamental state may be given with sufficient approximation by means of the linearized theory [11]. The prebuckling displacements are obtained from the linearized version of Eq. (8). In fact, by neglecting all the nonlinear terms, and applying the variational calculus, the differential equations of equilibrium are obtained and then are easily solved in a closed form in order to determine the initial displacements.

For the case of simply supported beams subjected to axial and uniform bending (see Fig. 2), the prebuckling displacements are given by the following expressions:

$$u_0 = \frac{P}{\widehat{EA}}(x - L), \tag{14}$$

$$w = \frac{Mo}{2\widehat{EI}_y\left(1 + \frac{P}{P_y}\right)}\left(Lx - x^2\right), \tag{15}$$

$$\theta_y = \frac{Mo\left(\widehat{GS}_z - P\right)}{2\widehat{EI}_y\widehat{GS}_z\left(1 + \frac{P}{P_y}\right)}(L - 2x), \tag{16}$$

where, $\widehat{EI}_y$ and $\widehat{GS}_z$ are the flexural and shear stiffnesses of a composite beam. $P_y$ represents the buckling axial load corresponding to bending mode (see Eq. (22)).

To determine the lateral buckling, considering prebuckling deformation, the initial displacements ((14)–(16)) are substituted into Exp. (8), the resultant variational equation is discretized by means of the trigonometric functions defined in Eq. (13) and then the tangential stiffness matrix is obtained [18]. This procedure leads to Eq. (17) (see Box I) for the tangential matrix evaluated in the fundamental state, where $\widehat{EI}_y$ is the flexural stiffness, $\widehat{GS}_z$ and $\widehat{GS}_y$ are shear stiffnesses of a composite beam. The definitions of these stiffnesses are given in the Appendix.

The buckling state is given by the condition of singularity of this matrix [18]:

$$\det(\mathbf{Kt}) = 0. \tag{18}$$

Therefore, a quadratic equation for the external loads are determined, the solution of which allows obtaining the critical values.

Following the same procedure for a distributed load and only changing the expression corresponding to the prebuckling displacement equations (14)–(16), it is possible to get a unified simple formula for the equivalent moment defined as:

$$M_{cr} = \begin{cases} M_{y0} & \text{for uniform bending} \\ q_z L^2/8 & \text{for a uniformly distributed load} \\ & \text{per unit length } q_z. \end{cases} \tag{19}$$

The explained technique leads to the following unified expression of the critical moment for both loading cases:

$$M_{cr} = C_1\frac{1}{\alpha}\frac{\pi^2}{L^2}\widehat{EI}_z\left(1 + \frac{P}{P_z}\right)\left(1 + \frac{P}{P_y}\right) \times \left[-C_2 e_z + \sqrt{\alpha\frac{I_0 L^2}{\widehat{EI}\pi^2}\frac{\left(P_\phi + P\right)}{\left(1 + \frac{P}{P_z}\right)\left(1 + \frac{P}{P_y}\right)} + (C_2 e_z)^2}\right], \tag{20}$$

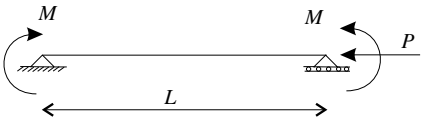


**Fig. 2.** Simply supported beams subjected to axial and uniform bending.

where

$$\alpha = \left(1 - \frac{\widehat{EI}_z}{\widehat{EI}_y}\right)\left(1 - \beta\frac{P_\phi I_0}{\widehat{EI}_y}\right)\left[1 + \left(P - 2.14\frac{P^2}{\widehat{GS}_z}\right) \times \left(-\frac{L^2}{3\widehat{EI}_y\pi^2} + \frac{1}{\widehat{GS}_y} - \frac{\eta}{\widehat{GS}_z}\left(1 - \frac{\widehat{EI}_z}{\widehat{EI}_y}\right)\right)\right] + \delta\frac{\widehat{EI}_z}{\widehat{GS}_y}\frac{\pi^2}{L^2}\left[1 - \frac{\widehat{GS}_y}{\widehat{GS}_z}\left(0.71 + \frac{\widehat{GS}_y}{\widehat{GS}_z}0.29\right)\right], \tag{21}$$

where, $I_0$ is the polar moment of inertia about shear center, and $C_1$, $C_2$, $\beta$ and $\delta$ are approximate constants presented in Table 1. It is worth noting that the axial load is in general considered positive in Exp. (14). In the case of compression load the load value is negative.

Furthermore, $P_y$, $P_z$, and $P_\phi$ are the buckling loads in bending and torsion of a simply supported composite beam subjected to an axial load [14].

$$P_z = \frac{\widehat{EI}_z\widehat{GS}_y\pi^2}{\widehat{GS}_y L^2 + \widehat{EI}_z\pi^2}, \tag{22}$$

$$P_y = \frac{\widehat{EI}_y\widehat{GS}_z\pi^2}{\widehat{GS}_z L^2 + \widehat{EI}_y\pi^2}, \tag{23}$$

$$P_\phi = \frac{L^2\widehat{GS}_w\widehat{GJ} + \widehat{EC}_w\pi^2\left(\widehat{GJ} + \widehat{GS}_w\right)}{I_0\left(\widehat{GS}_w L^2 + \widehat{EC}_w\pi^2\right)}. \tag{24}$$

The coefficient $\alpha$ represents the influence of the prebuckling deformation and depends mainly on the relation between the bending stiffnesses $\widehat{EI}_z$ and $\widehat{EI}_y$ in the case of uniform bending. For the other load condition, $\alpha$ also depends on the bending and shear stiffnesses ($\delta \neq 0$).

## 8. Effects of approximations on the buckling load analysis

In this section the effects of approximations in the analyses of thin-walled composite beams is studied for a simply supported beam subjected to uniform bending and axial load.

### *8.1. Neglecting the longitudinal displacements on the prebuckling deformation*

The first case corresponds to ignoring the influence of the axial displacements on the prebuckling deformation. Therefore, the initial displacements are given by the following expressions [11]:

$$w = \frac{Mo}{2\widehat{EI}_y}\left(Lx - x^2\right), \tag{25}$$

$$\theta_y = \frac{Mo}{2\widehat{EI}_y}(L - 2x). \tag{26}$$

Following the same procedure explained above, the expression for the tangential matrix yields Eq. (27) given in Box II. In this case, expression (20) takes the following form (Exp. (28)), which is obtained from the condition of singularity of the last matrix

$$\mathbf{Kt} = \begin{bmatrix} \left(\widehat{GS}_y + P\right)\frac{\pi^2}{L^2} & -\frac{\widehat{GS}_y\pi}{L} & 0 & 0 \\ & \widehat{GS}_y + \widehat{EI}_z\frac{\pi^2}{L^2} & -\left(Mo - \frac{P}{\widehat{GS}_z}\right)\left(1 - \frac{\widehat{EI}_z}{\widehat{EI}_y} - \frac{\widehat{GJ}}{4\widehat{EI}_y}\right)\frac{\pi}{L} & \frac{\widehat{EC}_w\pi^2 Mo}{4\widehat{EI}_y L^2} \\ & & -\frac{Mo^2}{\widehat{EI}_y\left(1+\frac{P}{P_y}\right)}\left(1 - \frac{\widehat{EI}_z}{\widehat{EI}_y}\right) + \left(\widehat{GJ} + \widehat{GS}_w\right)\frac{\pi^2}{L^2} + PI_0\frac{\pi^2}{L^2} & -\frac{\widehat{GS}_w\pi}{L} \\ \text{Sym} & & & \widehat{GS}_w + \widehat{EC}_w\frac{\pi^2}{L^2} \end{bmatrix} \tag{17}$$

**Box I.**

$$\mathbf{Kt} = \begin{bmatrix} \left(\widehat{GS}_y + P\right)\frac{\pi^2}{L^2} & -\frac{\widehat{GS}_y\pi}{L} & 0 & 0 \\ & \widehat{GS}_y + \widehat{EI}_z\frac{\pi^2}{L^2} & -Mo\left(1 - \frac{\widehat{EI}_z}{\widehat{EI}_y} - \frac{\widehat{GJ}}{4\widehat{EI}_y}\right)\frac{\pi}{L} & \frac{\widehat{EC}_w\pi^2 Mo}{4\widehat{EI}_y L^2} \\ & & -\frac{Mo^2}{\widehat{EI}_y}\left(1 - \frac{\widehat{EI}_z}{\widehat{EI}_y}\right) + \left(\widehat{GJ} + \widehat{GS}_w\right)\frac{\pi^2}{L^2} + PI_0\frac{\pi^2}{L^2} & -\frac{\widehat{GS}_w\pi}{L} \\ \text{Sym} & & & \widehat{GS}_w + \widehat{EC}_w\frac{\pi^2}{L^2} \end{bmatrix} \tag{27}$$

**Box II.**

**Table 1**
Parameters used in Eqs. (20)–(21).

| Simply supported beam | $C_1$ | $C_2$ | $\beta$ | $\delta$ | $\eta$ |
|---|---|---|---|---|---|
| (a) End moments | 1 | 0 | 0.5 | 0 | 4.0 |
| (b) Uniformly distributed load ($M_{cr} = q_z L^2/8$) | 1.141 | 0.459 | 0.033 | 0.214 | 0.071 |

(Exp. (27) as given in Box II), in the same way as was explained in the previous section.

$$M_{cr} = \frac{\sqrt{\widehat{EI}_z\frac{\pi^2}{L^2}I_o(P_\phi + P)\left(1 + \frac{P}{P_z}\right)}}{\sqrt{\left(1 - \frac{\widehat{EI}_z}{\widehat{EI}_y}\right)\left[\left(1 - \frac{P_\phi I_o}{2\widehat{EI}_y}\right)\left(1 + \frac{P}{\widehat{GS}_y}\right) + \frac{P}{\widehat{EI}_y}\frac{\pi^2}{L^2}\right]}}. \tag{28}$$

Comparing this last approximate formula with Eq. (20), for the case of bending moments, it is evident the absence of $P_y$, which represents the buckling loads in vertical flexural mode of a simply supported composite beam subjected to an axial load. Besides, the axial force term $P^2$ in the definition of $\alpha$ in Eq. (21) is not present in the denominator of Eq. (28).

### 8.2. Classical or linear theory

In this second case, the influence of the prebuckling displacements is neglected. This approximation is valid when the relation between out-of-plane flexural stiffness and torsional stiffness is small [19,20]. When the effects of in-plane prebuckling deformation are not considered, the analysis corresponds to a classical or linear approximation. Therefore, considering a problem of initial stresses and disregarding the initial deformation, the expression for the tangential matrix yields Eq. (29) given in Box III: In this case, Eq. (20) takes the following form:

$$M_{cr} = \sqrt{\frac{\widehat{EI}_z\frac{\pi^2}{L^2}I_o(P_\phi + P)\left(1 + \frac{P}{P_z}\right)}{1 + \frac{P}{\widehat{GS}_y}}}. \tag{30}$$

It is clear that the prebuckling term $\alpha$ is not present in this last approximate expression. The equivalent moments according to the linearized theory can be obtained from Eq. (20) by eliminating $P_y$ and considering:

$$\alpha = 1 + \frac{P}{\widehat{GS}_y}. \tag{31}$$

### 8.3. Without shear deformation

The influence of shear deformation can be neglected for slender beams or for some particular stacking sequences where the ratio between the equivalent elasticity modulus and the transverse elasticity modulus is low. The reduced form of the buckling load is the same as Eq. (20), however the definition of $\alpha$ in Eq. (21) takes the following form:

$$\alpha = \left(1 - \frac{\widehat{EI}_z}{\widehat{EI}_y}\right)\left(1 - \beta\frac{P_\phi I_0}{\widehat{EI}_y}\right)\left(1 - \frac{PL^2}{3\widehat{EI}_y\pi^2}\right). \tag{32}$$

Finally, the expressions of the buckling loads in bending and torsion of a simply supported composite beam subjected to an axial load are obtained by neglecting shear stiffnesses from Eqs. (22)–(24). It is assumed that shear stiffnesses ($\widehat{GS}_y$, $\widehat{GS}_z$ and $\widehat{GS}_w$) are extremely larger than bending and warping stiffnesses ($\widehat{EI}_y$, $\widehat{EI}_z$ and $\widehat{EC}_w$). Therefore, the buckling load yields:

$$P_z = \widehat{EI}_z\frac{\pi^2}{L^2}, \tag{33}$$

$$P_y = \widehat{EI}_y\frac{\pi^2}{L^2}, \tag{34}$$

$$\mathbf{Kt} = \begin{bmatrix} \left(\widehat{GS}_y + P\right)\frac{\pi^2}{L^2} & -\frac{\widehat{GS}_y\pi}{L} & 0 & 0 \\ & \widehat{GS}_y + \widehat{EI}_z\frac{\pi^2}{L^2} & -Mo\frac{\pi}{L} & 0 \\ & & \left(\widehat{GJ} + \widehat{GS}_w\right)\frac{\pi^2}{L^2} + PI_0\frac{\pi^2}{L^2} & -\frac{\widehat{GS}_w\pi}{L} \\ \text{Sym} & & & \widehat{GS}_w + \widehat{EC}_w\frac{\pi^2}{L^2} \end{bmatrix} \tag{29}$$

**Box III.**

$$P_\phi = \frac{L^2\widehat{GJ} + \widehat{EC}_w\pi^2}{I_0L^2}. \tag{35}$$

### 8.4. Comparison with existing solutions

As was pointed out in the Introduction of this paper, there is no publication available that consider the effects of shear and prebuckling deformation on the stability response analysis of the thin-walled composite beams under combined axial and bending loads. Recently Mohri et al. [15] presented a compact closed-form solution for the buckling loads of a simply supported beam–column non-shear deformable steel elements. The analytical expression includes first-order bending distribution, load height level, prebuckling deflection effects and the presence of axial loads. The buckling moments expression derived by Mohri et al. [15] is shown in Eq. (36).

$$M_{0,b} = C_1\frac{\pi^2}{L^2}EI_z\left[C_2e_z \pm \sqrt{\frac{I_w}{I_z}\left(1 + \frac{GJL^2}{EC_w\pi^2}\right) + (C_2e_z)^2}\right] \times \sqrt{\left(1 - \frac{P}{P_y}\right)\left(1 - \frac{P}{P_z}\right)\left(1 - \frac{P}{P_\theta}\right)}, \tag{36}$$

where, the coefficients $C_1$ and $C_2$ used in Eq. (36) are the following:

$$C_1 = \frac{1.14}{\sqrt{1 - \frac{I_z}{I_y}}}, \qquad C_2 = \frac{0.46}{\sqrt{1 - \frac{I_z}{I_y}}}\left(1 - \frac{P}{P_y}\right)\left(1 - \frac{P}{P_z}\right)\left(1 - \frac{P}{P_\theta}\right)^{-1}. \tag{37}$$

In order to compare these last expressions with the present ones, the coefficients $C_1$ and $C_2$ are substituted into Eq. (36) and after some arrangements the resultant expression becomes:

$$M_{0,b} = 1.14\frac{\pi^2}{L^2}\frac{EI_z}{\left(1 - \frac{I_z}{I_y}\right)}\left(1 - \frac{P}{P_z}\right)\left(1 - \frac{P}{P_y}\right)\left[-0.46e_z + \sqrt{\frac{\left(1 - \frac{I_z}{I_y}\right)\frac{I_w}{I_z}\left(1 + \frac{GJL^2}{EC_w\pi^2}\right)}{\left(1 - \frac{P}{P_y}\right)\left(1 - \frac{P}{P_z}\right)\left(1 - \frac{P}{P_\theta}\right)^{-1}} + (0.46e_z)^2}\right]. \tag{38}$$

This last expression, developed by Morhi et al. [15], is very similar to Eq. (20) developed in the present article. The only difference is in the definition of the coefficient $\alpha$, which represents the prebuckling deformation. In the present formulation $\alpha$ is represented by Eq. (32), while in the case of Morhi et al. [15] solution $\alpha$ yields:

$$\alpha = 1 - \frac{I_z}{I_y}. \tag{39}$$

**Table 2**
Materials considered in the numerical applications.

| Properties | Glass/epoxy (M1) | Graphite/epoxy (M2) |
|---|---|---|
| *Young's modules* (GPa) | | |
| $E_1$ | 48.3 | 144 |
| $E_2$ | 19.8 | 9.65 |
| *Shear's modules* (GPa) | | |
| $G_{12} = G_{13}$ | 8.96 | 4.14 |
| $G_{23}$ | 6.19 | 3.45 |
| *Poisson's ratio* | | |
| $\nu_{12} = \nu_{13}$ | 0.27 | 0.3 |
| $\nu_{23}$ | 0.60 | 0.5 |

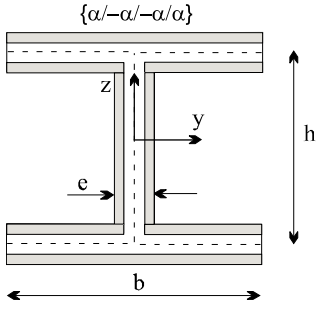


**Fig. 3.** Four layered composite cross-section.

In order to know a little more about this coefficient, the effects of shear deformation, load height level and the presence of axial loads are neglected in Eq. (20). Therefore, Eq. (20) is reduced to the following form:

$$M_{cr} = 1.14\frac{1}{\alpha}\frac{\pi}{L}\sqrt{\alpha EI_z\left(GJ + EC_w\frac{\pi^2}{L^2}\right)}, \tag{40}$$

$$\alpha = \left(1 - \frac{I_z}{I_y}\right)\left(1 - \beta\frac{GJ}{EI_y} - \beta\frac{EC_w}{EI_y}\frac{\pi^2}{L^2}\right). \tag{41}$$

These last expressions agree with the closed-form solution obtained by Pi and Trahair [9] for elastic lateral buckling, of beams made with isotropic materials, considering prebuckling deflections. It is clear that the prebuckling effect considered in the Pi and Trahair solution [9] is the same as in the present formulation.

## 9. Applications and numerical results

The purpose of this section is to apply the present method in order to study the lateral stability behavior of thin-walled composite beams under combined axial and lateral loads. The numerical results are obtained for a four layer bisymmetric-I cross-section (Fig. 3). Material properties corresponding to S2-glass/epoxy (M1) and AS4/3501 graphite/epoxy (M2) are defined in Table 2.

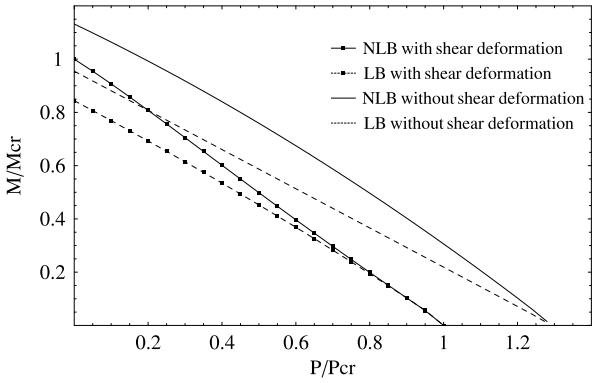


**Fig. 4.** Buckling load of a beam under combined axial and end moments, for a sequence {0/0/0/0}.

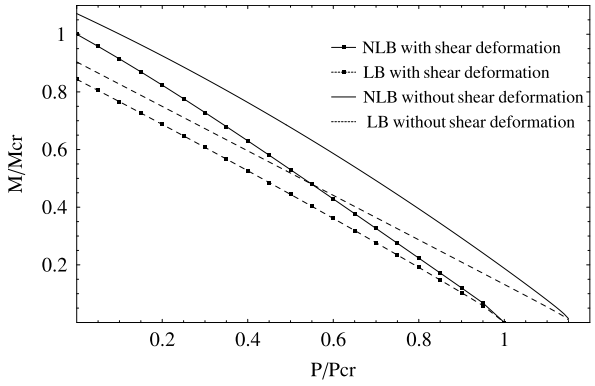


**Fig. 5.** Buckling load of a beam under combined axial and end moments, for a sequence {0/90/90/0}.

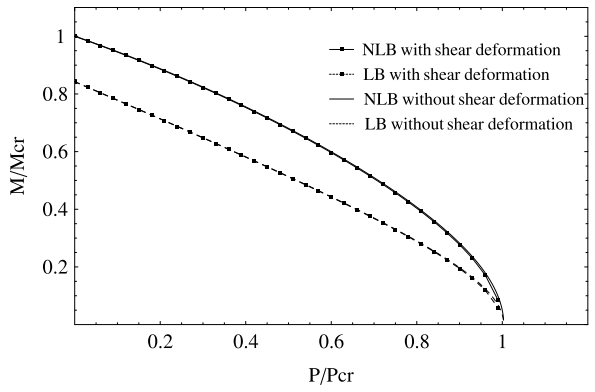


**Fig. 6.** Buckling load of a beam under combined axial and end moments, for a sequence {45/−45/−45/45}.

### 9.1. Simply supported I-beam subjected to uniform moments

The example considered is a simply supported I-beam subjected to axial force and uniform bending moment *Mo* applied about its major axis as shown in Fig. 2. The geometrical properties are $h = 0.6$ m, $b = 0.6$ m, $e = 0.03$ m, $L = 6$ m and the analyzed material is graphite–epoxy.

The effect of prebuckling deformation on the lateral buckling is shown in Figs. 4–6, for a sequence of lamination {0/0/0/0}, {0/90/90/0} and {45/−45/−45/45}, respectively. The analytical buckling moments considering and neglecting the prebuckling deflections were calculated by means of Eqs. (20)–(21) along with Table 1, and by means of Eqs. (30)–(31), respectively. In the figures and tables, the buckling values determined by the linear theory (without considering prebuckling deformations) are denoted by *LB* and the values obtained by means of the present model with *NLB* (accounting for prebuckling deflections). The critical loads computed by Eq. (28), which is without longitudinal displacements on the prebuckling deformation, are denoted by *NLP*. The bending load $M$ is scaled with the value of the critical load considering the axial load $P = 0$ ($M_{cr}$ for the *NLB* model). In the same way, the axial load $P$ is scaled with the first critical load value corresponding to the case of $M = 0$ ($P_{cr} = P_z$). The buckling loads for some particular cases are shown in Table 3.

The buckling moments computed from the linear stability (*LB*) analysis present a very conservative behavior compared with those computed from the nonlinear stability (*NLB*) analysis. The numerical results corresponding to the *NLP* model (Eq. (28)), overestimates the buckling load for the lamination sequences {0/0/0/0} and {0/90/90/0}, while underestimates the critical load for a lamination {45/−45/−45/45}. Moreover, the influence of the geometrically nonlinear effect on the lateral buckling loads decreases as the moment ratio $M/M_{cr}$ and the prebuckling deformation decrease, and it is larger when there is no axial load. The lamination {0/0/0/0} presents the higher critical loads in all the cases analyzed. On the other hand, the shear deformation effect reduces significantly the buckling load values. This effect is larger for unidirectional fibers and insignificant for the sequence of lamination {45/−45/−45/45}. For this last lamination the curves with and without shear deformation coincide for both analyses (*NLB* and *LB*).

The buckling loads computed with the present model and those obtained by using the classical theory *LB* without shear deformation agree in some cases. For example, for a ratio $P/P_{cr} = 0.2$ and a sequence of lamination {0/0/0/0} (see Fig. 4), both formulations present $M_{cr} = 10.97$ MN m. The same behavior is observed for the sequence of lamination {0/90/90/0} (see Fig. 5), where the same buckling moment is obtained for $P/P_{cr} = 0.55$ ($M_{cr} = 3.70$ MN m).

When the beam is loaded in the vertical plane, the displacements of this situation correspond to the prebuckling state, and then at a certain level of the applied load, the beam may buckle laterally, while the cross-sections of the beam rotate simultaneously about the beam's axis. When the buckling load is reached, the behavior of the beam is initially flexural–torsional and corresponds to the secondary or equilibrium path. In order to investigate the precision of the analytical buckling moments, the postbuckling response is analyzed for different axial load values. The initial postbuckling paths corresponding to the displacement amplitudes $u_0$, $v$, $w$ and $\phi$ are shown in Figs. 7 and 8, for an axial load $P = 0$ and $P = 0.5P_{cr}$, respectively. In both cases the postbuckling equilibrium paths are stable and symmetric. The numerical bifurcations observed in the figures agree with the buckling loads obtained by means of the analytical closed-form solutions shown in Table 3. The initial postbuckling curves are similar for both load cases. However, when the beam is subjected to the axial load the prebuckling curves have a stiffer behavior.

### 9.2. Influence of the cross-section on the prebuckling behavior

The influence of the cross-section on the geometrically nonlinear effects is analyzed in this example. The beam is subjected to the same load conditions as that in the previous section. In this case, the width of the flanges is decreased to the value of $b = 0.3$ m, while the other cross-section dimensions and material are the same. The sequence of lamination used is {0/90/90/0} and the beam length is $L = 4$ m.

The variations of buckling loads are shown in Fig. 9, where the critical values obtained by the present nonlinear formulation are compared with the classical predictions. In comparison with the previous example, the discrepancy between both formulations, due to the prebuckling deformations, is lower. This behavior is

**Table 3**
Buckling loads considering different models ($M_{cr} \times 10^6$ N m).

| Load | Buckling analysis | {0/0/0/0} | {0/90/90/0} | {45/−45/−45/45} |
|---|---|---|---|---|
| | $P_z$ | 33.18 | 19.83 | 4.43 |
| $M = 0$ | $P_\phi$ | 33.93 | 20.58 | 8.51 |
| | $P_y$ | 49.71 | 38.59 | 15.21 |
| $P = 0$ | $M_{cr}$ | 13.53 | 7.71 | 2.19 |
| | *NLB* | 6.74 | 4.09 | 1.49 |
| $P = 0.5P_{cr}$ | *NLB without shear* | 10.27 | 5.22 | 1.49 |
| | *LB* | 6.12 | 3.42 | 1.12 |
| | *LB without shear* | 7.94 | 4.00 | 1.13 |
| | *NLP* | 7.75 | 4.36 | 1.44 |

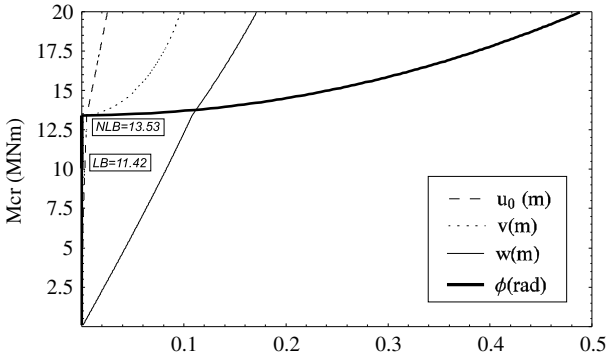


**Fig. 7.** Postbuckling response of a beam under end moments, for a sequence {0/0/0/0}.

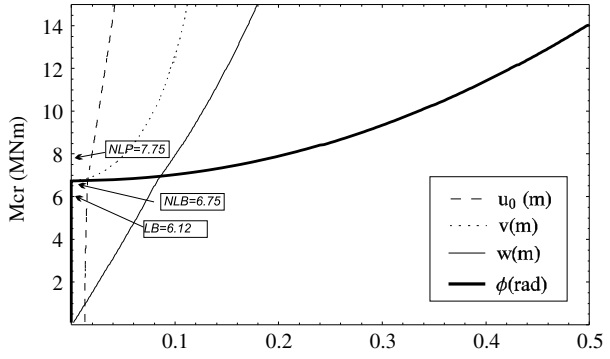


**Fig. 8.** Postbuckling response of a beam under end moments and axial force $P = 0.5P_{cr}$, for a sequence {0/0/0/0}.

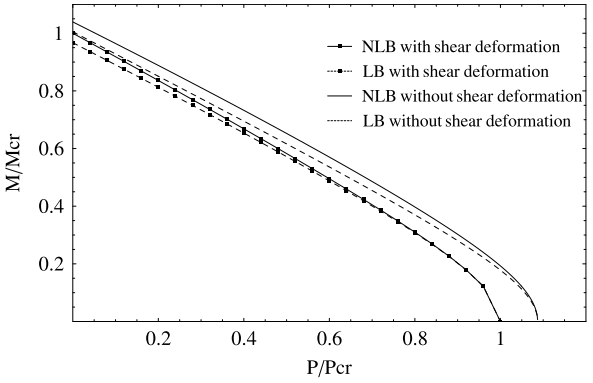


**Fig. 9.** Lateral buckling resistance influenced by an axial force, for a sequence {0/90/90/0}.

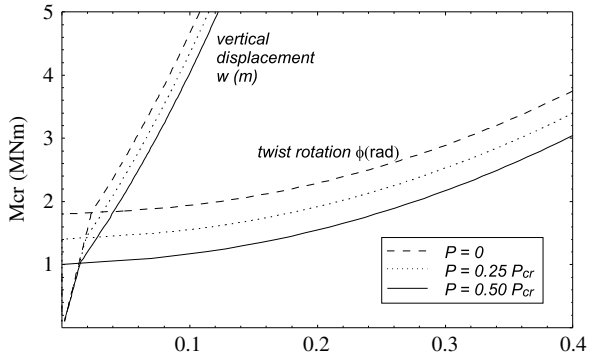


**Fig. 10.** Influence of the axial force on prebuckling and initial postbuckling paths.

due to the relation between the flexural stiffnesses. In this case the ratio is $\widehat{EI}_z/\widehat{EI}_y = 0.063$, while in the previous section it was $\widehat{EI}_z/\widehat{EI}_y = 0.286$. The value of $\alpha$ approximates to one when this relation decreases (considering an axial force $P = 0$) and Eqs. (20) and (30) become similar.

The load–displacement curves are shown in Fig. 10, for three axial force cases. The stability behavior is represented by the vertical displacement $w$ (corresponding to the load in-plane movement) and by the torsional twist $\phi$ (corresponding to the postbuckling response). The axial load effect reduces considerably the values of the equilibrium path curves, which are stable and symmetric. This decrease is proportional to the increase of the axial load. This effect keeps constant for large displacement values on the equilibrium path.

### 9.3. Simply supported I-beam subjected to distributed load

A simply supported I-beam under a combined axial and distributed load is analyzed. The distributed load can be applied to the top flange, on the shear center, and to the bottom flange (see Fig. 11). Therefore, the load height parameter effect on the buckling and postbuckling behavior can be analyzed. The cross-sections are the same as that in the previous example and the beam length is $L = 6$ m. In this case, two composite materials are considered in the analysis (see Table 2); the stacking sequence {0/0/0/0} is considered.

The load–twisting curves are shown in Figs. 12 and 13, corresponding to graphite/epoxy and glass/epoxy materials, respectively. The bifurcation point depends on the load height parameter and the axial load. In Table 4, the numerical bifurcation loads are compared with the analytical buckling loads obtained by means of Eq. (20). The buckling values obtained with the analytical expression are, in general, in good agreement with the bifurcation loads observed in Figs. 12 and 13. There is a little discrepancy between both models for the stiffer case, e.g., when the load is applied on the bottom flange for graphite/epoxy material and $P = 0$.

The effect of the axial load reduces the bifurcation points and the equilibrium curve values. The influence of this effect is larger when the distributed load is applied on the bottom flange and is smaller for the load applied on the top flange (the lowest buckling load case). Furthermore, comparing both materials, it can be observed that the stability behavior is similar and the load axial effect is higher when the graphite/epoxy material is employed.

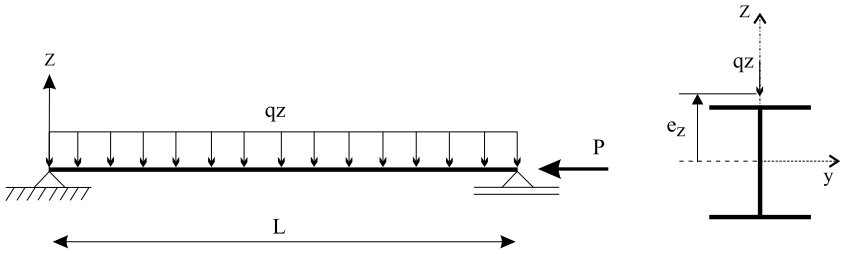


**Fig. 11.** Simply supported beam subjected to combined axial and distributed loads applied in different heights.

**Table 4**
Comparison of buckling loads $q_z$ (MN/m).

| Axial load | Load height | Material graphite/epoxy | | Material glass/epoxy | |
|---|---|---|---|---|---|
| | | Numerical (Fig. 12) | Exp. (20) | Numerical (Fig. 12) | Exp. (20) |
| $P = 0$ | $e_z = h/2$ | 0.25 | 0.27 | 0.12 | 0.12 |
| | $e_z = 0$ | 0.42 | 0.42 | 0.18 | 0.18 |
| | $e_z = -h/2$ | 0.92 | 0.67 | 0.27 | 0.26 |
| $P = 0.5P_{cr}$ | $e_z = h/2$ | 0.15 | 0.17 | 0.08 | 0.08 |
| | $e_z = 0$ | 0.25 | 0.26 | 0.11 | 0.11 |
| | $e_z = -h/2$ | 0.40 | 0.41 | 0.15 | 0.16 |

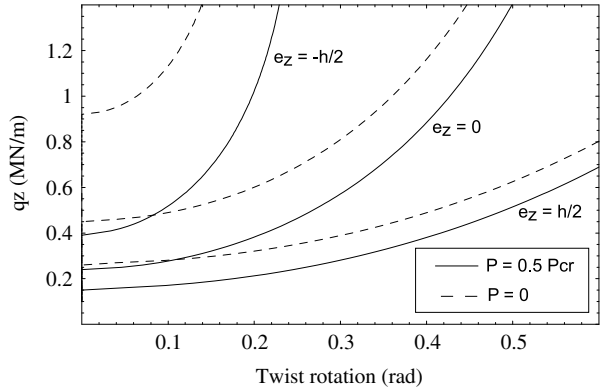


**Fig. 12.** Influence of the load height parameter on the postbuckling curves, Graphite/epoxy material.

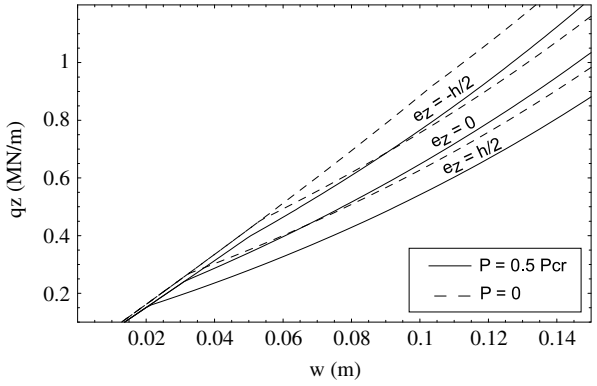


**Fig. 14.** Influence of the load height parameter on the prebuckling displacements, Graphite/epoxy material.

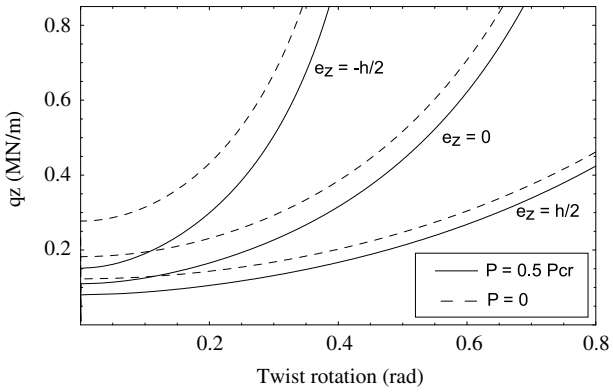


**Fig. 13.** Influence of the load height parameter on the postbuckling curves, Glass/epoxy material.

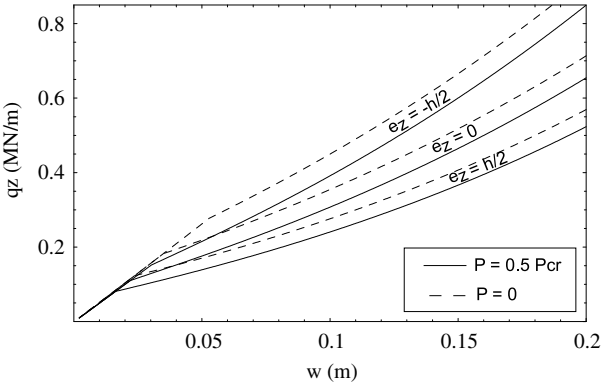


**Fig. 15.** Influence of the load height parameter on the prebuckling displacements, Glass/epoxy material.

On the other hand, the load–deflection curves $w$, corresponding to the prebuckling and postbuckling paths, are shown in Figs. 14 and 15, considering graphite/epoxy and glass/epoxy materials, respectively. The axial load effect reduces the prebuckling displacement and this effect is more significant when the load is applied on the bottom flange, the same behavior observed in the buckling and the postbuckling response. The reduction in the postbuckling curve values is larger when the graphite/epoxy material is used (see Fig. 14). Finally, the smaller prebuckling displacement corresponds to the glass/epoxy material, when the beam is subjected to a combined axial and distributed load applied on the top flange (see Fig. 15).

### 9.4. Comparison with existing solutions

For verification purposes, an isotropic simply supported beam subjected to a combined axial and distributed load is considered. The material properties are assumed to be $E = 210$ GPa and

**Table 5**
Lateral buckling moments of isotropic beams for various loading cases ($M_{cr} \times 10^6$ N m).

| Load height | $P/P_{cr}$ | Numeric (Abaqus) Ref. [15] | Analytic Ref. [15] | Present with shear Eqs. (20) and (21) | Present without shear Eqs. (20) and (32) | Analytic Eq. (38) |
|---|---|---|---|---|---|---|
| | 0.0 | 118.13 | 119.88 | 121.23 | 122.16 | 121.80 |
| $e_z = h/2$ | 0.2 | 98.73 | 101.97 | 102.51 | 103.43 | 102.92 |
| | 0.5 | 74.81 | 75.25 | 74.32 | 75.07 | 74.36 |
| | 0.75 | 49.55 | 50.51 | 49.52 | 49.52 | 48.80 |
| | 0.0 | 238.97 | 241.33 | 237.27 | 237.32 | 240.44 |
| $e_z = -h/2$ | 0.2 | 190.22 | 191.64 | 189.57 | 189.60 | 188.84 |
| | 0.5 | 124.20 | 124.88 | 119.84 | 119.85 | 119.88 |
| | 0.75 | 71.64 | 72.33 | 68.95 | 68.96 | 68.36 |

$G = 80.77$ GPa. The geometrical properties of the I-beam are $h = 0.195$ m, $b = 0.2$ m, $L = 6$ m and the thicknesses of the flange and the web are 0.01 m and 0.0065 m, respectively.

The results using the present analysis are compared with previously available results [15] in Table 5, for various loading conditions. The numerical simulations presented in Ref. [15] correspond to a shell finite element formulation (S8R5) obtained by means of Abaqus code. The numerical buckling loads were obtained following the fundamental path of the nonlinear behavior of the beam. The lateral buckling moments obtained with the analytical solution (Eq. (38)) developed by Mohri et al. [15], are shown in Table 5. The analytical solutions have been validated for different values of the axial load $P$, respectively, equal to 0.0, $0.2P_{cr}$, $0.5P_{cr}$ and $0.75P_{cr}$. The axial critical load obtained by Mohri et al. [15], for a simply supported beam–column non-shear deformable steel elements, is $P_z = 767.64$ kN (Eq. (33)). While the buckling load obtained with the present model is $P_z = 766.05$ kN (Eq. (22)). The difference between both models is due to the shear deformation effect.

It is seen that the results of the present formulation are in good agreement with the results presented in Ref. [15]. It is important to notice that the moments computed from Eq. (38) present a little discrepancy with those presented as analytic in Ref. [15].

This discrepancy can be due to how the sectional characteristics are computed.

## 10. Conclusions

In this paper the stability of thin-walled composite beam subjected to combined axial and lateral loads has been analyzed. Analytical solutions for the buckling load of simply supported beam are obtained and compared with the numerical results. The model used to obtain the analytical expressions is based on a geometrically nonlinear formulation which incorporates some non-conventional aspects. The effects of shear flexibility, higher-order bending–torsional coupling and warping stiffness are taken into account in the beam model. The theory is formulated in the context of large displacements and rotations, considering moderate bending rotations and large twist. Composite is assumed to be made of symmetric balanced laminates and especially orthotropic laminates. The effect of approximations in lateral buckling analysis of thin-walled beams is analyzed. Approximate analytical expressions are obtained to study the influence of axial load on the prebuckling displacements, shear deformation and the geometrically nonlinear effects of a simply supported beam subjected to combined axial and bending loads.

The buckling loads obtained analytically are, in general, in good agreement with the bifurcation loads observed in the postbuckling response. The comparison with available results was satisfactory. Therefore, the present closed-form solution is appropriate for predicting lateral buckling loads.

The effect of combined load reduces the lateral buckling load. The inclusion of the right prebuckling displacement is essential to get an accurate buckling load. The buckling moments computed from the classical theory present a very conservative behavior. The influence of this geometrically nonlinear effect decreases when the axial load increases. On the other hand, when the axial load is neglected in the prebuckling displacements, the lateral buckling load value is overestimated.

The initial postbuckling curves are stable and symmetric in all the cases analyzed. The values corresponding to the equilibrium path are reduced with the influence of the axial load. The shapes of the postbuckling curves are similar with the effect of the axial load. However, the curves corresponding to the prebuckling displacement have a stiffer behavior when the beam is subjected to the combined load case. It is well known that the buckling and the postbuckling behavior are influenced by the fiber orientation of the composite material. In this case, the effect of axial load is larger when the fibers are oriented in the longitudinal direction $\{0/0/0/0\}$. Finally, from the analysis of the load height parameter effect, on the buckling and the postbuckling response, it is demonstrated that the combined load effect is larger for the stiffest load condition, which is when the lateral load is applied on the bottom beam flange.

## Acknowledgements

The present study was sponsored by Secretaría de Ciencia y Tecnología, Universidad Tecnológica Nacional, and by CONICET (Consejo Nacional de Investigaciones Científicas y Técnicas).

## Appendix

The constitutive relations between the generalized forces and generalized strains are expressed, for a bisymmetric beam, in the form Eqs. (A.1)–(A.3) as given in Box IV, where $\{f_g\}$ is the vector of generalized forces, $\{\Delta\}$ is the vector of the generalized strains and $[K]$ is a symmetric matrix $(12 \times 12)$ (see Box V).

$$\varepsilon_{D1} = u_o' + \frac{1}{2}\left(u_o'^2 + v'^2 + w'^2\right) + \left(z_0\theta_z' - y_0\theta_y'\right)\sin\phi,$$

$$\varepsilon_{D2} = \left(-\theta_y' - u_o'\theta_y'\right)\cos\phi + \left(\theta_z' + u_o'\theta_z'\right)\sin\phi,$$

$$\varepsilon_{D3} = \left(-\theta_z' - u_o'\theta_z'\right)\cos\phi - \left(\theta_y' + u_o'\theta_y'\right)\sin\phi,$$

$$\varepsilon_{D4} = \theta' - \frac{1}{2}\left(\theta_z\theta_y'' - \theta_y\theta_z''\right),$$

$$\varepsilon_{D5} = \left(v' - \theta_z - u_0'\theta_z\right)\cos\phi - z_0\frac{1}{2}\left(\theta_z\theta_y' - \theta_y\theta_z'\right) + \left(w' - \theta_y - u_0'\theta_y\right)\sin\phi,$$

$$\varepsilon_{D6} = \left(w' - \theta_y - u_0'\theta_y\right)\cos\phi + y_0\frac{1}{2}\left(\theta_z\theta_y' - \theta_y\theta_z'\right) - \left(v' - \theta_z - u_0'\theta_z\right)\sin\phi,$$

$$\varepsilon_{D7} = \phi' - \theta,$$

$$\varepsilon_{D8} = \phi' - \frac{1}{2}\left(\theta_z\theta_y' - \theta_y\theta_z'\right),$$

$$\{f_g\} = [K]\{\Delta\} \tag{A.1}$$

$$\{f_g\} = \begin{bmatrix} N & M_y & M_z & B & Q_y & Q_z & T_w & T_{sv} & B_1 & P_{yy} & P_{zz} & P_{yz} \end{bmatrix}^T \tag{A.2}$$

$$\{\Delta\} = \begin{bmatrix} \varepsilon_{D1} & \varepsilon_{D2} & \varepsilon_{D3} & \varepsilon_{D4} & \varepsilon_{D5} & \varepsilon_{D6} & \varepsilon_{D7} & \varepsilon_{D8} & \varepsilon_{D9} & \varepsilon_{D10} & \varepsilon_{D11} & \varepsilon_{D12} \end{bmatrix}^T \tag{A.3}$$

**Box IV.**

$$K = \begin{bmatrix} \widehat{EA} & 0 & 0 & 0 & 0 & 0 & 0 & 0 & \widehat{EI}_0 & K_{1,10} & K_{1,11} & K_{1,12} \\ & \widehat{EI}_y & 0 & 0 & 0 & 0 & 0 & 0 & 0 & 0 & 0 & 0 \\ & & \widehat{EI}_z & 0 & 0 & 0 & 0 & 0 & 0 & 0 & 0 & 0 \\ & & & \widehat{EC}_w & 0 & 0 & 0 & 0 & 0 & 0 & 0 & K_{4,12} \\ & & & & \widehat{GS}_y & 0 & 0 & 0 & 0 & 0 & 0 & 0 \\ & & & & & \widehat{GS}_z & 0 & 0 & 0 & 0 & 0 & 0 \\ & & & & & & \widehat{GS}_w & 0 & 0 & 0 & 0 & 0 \\ & & & & & & & \widehat{GJ} & 0 & 0 & 0 & 0 \\ & & & & & & & & \widehat{EI}_R & K_{9,10} & K_{9,11} & K_{9,12} \\ & & \text{Sym} & & & & & & & K_{10,10} & K_{10,11} & K_{10,12} \\ & & & & & & & & & & K_{11,11} & K_{11,12} \\ & & & & & & & & & & & K_{12,12} \end{bmatrix} \tag{A.5}$$

**Box V.**

$$\widehat{EA} = \int \bar{A}_{11}\mathrm{d}s \qquad K_{1,12} = \int \bar{A}_{11}\bar{Y}\bar{Z}\mathrm{d}s$$

$$\widehat{EI}_y = \int \left(\bar{A}_{11}Z^2 + \bar{D}_{11}Y'^2\right)\mathrm{d}s \qquad K_{4,12} = \int \left[\bar{A}_{11}\bar{Y}\omega_p\bar{Z} - \bar{D}_{11}\left(\bar{Y}Y' - \bar{Z}Z'\right)l\right]\mathrm{d}s$$

$$\widehat{EI}_z = \int \left(\bar{A}_{11}Y^2 + \bar{D}_{11}Z'^2\right)\mathrm{d}s \qquad K_{9,10} = \int \left[\bar{A}_{11}\left(Y^2+Z^2\right)\bar{Z}^2 - 4\bar{D}_{11}\bar{Z}Y'r\right]\mathrm{d}s$$

$$\widehat{EI}_w = \int \left(\bar{A}_{11}\omega_p^2 + \bar{D}_{11}l^2\right)\mathrm{d}s \qquad K_{9,11} = \int \left[\bar{A}_{11}\left(Y^2+Z^2\right)\bar{Y}^2 + 4\bar{D}_{11}\bar{Y}Z'r\right]\mathrm{d}s$$

$$\widehat{GS}_y = \int \left(\bar{A}_{55}Z'^2 + \bar{A}_{66}Y'^2\right)\mathrm{d}s \qquad K_{9,12} = \int \left[\bar{A}_{11}\left(Y^2+Z^2\right)\bar{Y}\bar{Z} - 2\bar{D}_{11}\left(\bar{Y}Y' - \bar{Z}Z'\right)r\right]\mathrm{d}s$$

$$\widehat{GS}_z = \int \left(\bar{A}_{55}Y'^2 + \bar{A}_{66}Z'^2\right)\mathrm{d}s \qquad K_{10,10} = \int \left(\bar{A}_{11}\bar{Z}^4 + 4\bar{D}_{11}\bar{Z}^2Y'^2\right)\mathrm{d}s \tag{A.6}$$

$$\widehat{GJ} = \int \left(\bar{A}_{66}\psi^2 + 4\bar{D}_{66}\right)\mathrm{d}s \qquad K_{10,11} = \int \left(\bar{A}_{11}\bar{Z}^2\bar{Y}^2 - 4\bar{D}_{11}\bar{Z}Y'\bar{Y}Z'\right)\mathrm{d}s$$

$$\widehat{EI}_R = \int \left[\bar{A}_{11}\left(Y^2+Z^2\right)^2 + 4\bar{D}_{11}r^2\right]\mathrm{d}s \qquad K_{10,12} = \int \left[\bar{A}_{11}\bar{Z}^3\bar{Y} + 2\bar{D}_{11}\left(\bar{Y}Y' - \bar{Z}Z'\right)\bar{Z}Y'\right]\mathrm{d}s$$

$$\widehat{EI}_0 = \int \bar{A}_{11}\left(Y^2+Z^2\right)\mathrm{d}s \qquad K_{11,11} = \int \left(\bar{A}_{11}\bar{Y}^4 - 4\bar{D}_{11}\bar{Y}^2Z'^2\right)\mathrm{d}s$$

$$K_{1,10} = \int \bar{A}_{11}\bar{Z}^2\mathrm{d}s \qquad K_{10,12} = \int \left[\bar{A}_{11}\bar{Y}^3\bar{Z} - 2\bar{D}_{11}\left(\bar{Y}Y' - \bar{Z}Z'\right)\bar{Y}Z'\right]\mathrm{d}s$$

$$K_{1,11} = \int \bar{A}_{11}\bar{Y}^2\mathrm{d}s \qquad K_{12,12} = \int \left[\bar{A}_{11}\bar{Z}^2\bar{Y}^2 + \bar{D}_{11}\left(\bar{Y}Y' - \bar{Z}Z'\right)^2\right]\mathrm{d}s$$

**Box VI.**

$$\varepsilon_{D9} = \frac{\phi'^2}{2},$$
$$\varepsilon_{D10} = \frac{\theta_y'^2}{2},$$
$$\varepsilon_{D11} = \frac{\theta_z'^2}{2},$$
$$\varepsilon_{D12} = \theta_y'\theta_z'. \tag{A.4}$$

The elements of the symmetric matrix $[K]$ are given by the contour integrals (see Box VI), where

$$Y' = \frac{\mathrm{d}Y}{\mathrm{d}s}; \qquad Z' = \frac{\mathrm{d}Z}{\mathrm{d}s}. \tag{A.7}$$

## References


[1] Vlasov VZ. Thin walled elastic beams. Jerusalem: Israel Program for Scientific Translation; 1961.
[2] Timoshenko SP, Gere JM. Theory of elastic stability. 2nd ed. New York: McGraw-Hill; 1961.
[3] Bleich F. Buckling strength of metal structures. New York: McGraw-Hill; 1952.
[4] Chajes A. Principle of structural stability theory. Englewood Cliffs, NJ: Prentice-Hall; 1952.
[5] Goodier JN. The buckling of compressed bars by torsion and flexure. Bulletin 27. Cornell University Engineering Experimental Station; 1941.
[6] Sapkás A, Kollár LP. Lateral–torsional buckling of composite beams. Internat J Solids Structures 2002;39:2939–63.
[7] Lee J, Kim SE, Hong K. Lateral buckling of I-section composite beams. Eng Struct 2002;24:955–64.
[8] Vacharajittiphan P, Woolcock ST, Trahair NS. Effect of in-plane deformation on lateral buckling. J Struct Mech 1974;3(1):29–60.
[9] Pi YL, Trahair NS. Prebuckling deflections and lateral buckling. II: applications. J Struct Eng, ASCE 1992;118(11):2967–85.

[10] Mohri F, Azrar L, Potier-Ferry M. Lateral post-buckling analysis of thin-walled open sections beams. Thin-Walled Struct 2002;40:1013–36.
[11] Machado SP, Cortínez VH. Lateral buckling of thin walled composite bisymmetric beams with prebuckling and shear deformation. Eng Struct 2005; 27:1185–96.
[12] Machado SP, Cortínez VH. Non-Linear model for stability of thin walled composite beams with shear deformation. Thin-Walled Struct 2005;43: 1615–45.
[13] Sapountzakis EJ, Panagos DG. Shear deformation effect in non-linear analysis of composite beams of variable cross section. Internat J Non-Linear Mech 2008; 43:660–82.
[14] Machado SP. Non-linear buckling and postbuckling behavior of thin-walled beams considering shear deformation. Internat J Non-Linear Mech 2008;43: 345–65.
[15] Mohri F, Bouzerira C, Potier-Ferry M. Lateral buckling of thin-walled beam–column elements under combined axial and bending loads. Thin-Walled Struct 2008;46:290–302.
[16] Barbero EJ. Introduction to composite material design. Taylor and Francis Inc.; 1999.
[17] Cortínez VH, Piovan MT. Vibration and buckling of composite thin-walled beams with shear deformability. J Sound Vib 2002;258:701–23.
[18] Bazant ZP, Cedolin L. Stability of structures: elastic, inelastic, fracture, and damage theories. Mineola, New York: Dover Publication, Inc.; 2003.
[19] Pi YL, Bradford MA. Effects of approximations in analysis of beams of open thin-walled cross-section—part II: 3-D non-linear behavior. Internat J Numer Methods Engrg 2001;51:773–90.
[20] Machado SP. Geometrically non-linear approximations on stability and free vibration of composite beams. Eng Struct 2007;29:3567–78.